Environmental and Microbial Technology
https://www.sciltp.com/journals/emt

Review

Machine Learning Assists in the Design of Photocatalysts for Environmental Remediation: A Comprehensive Review

Wei Liu, Bingqing Wang, Danzeng Yangjin and Sihui Zhan *

School of Environmental Science and Engineering, Tianjin University, No. 92 Weijin Road, Nankai District, Tianjin 300072, China
* Correspondence: shzhan@tju.edu.cn

How To Cite: Liu, W.; Wang, B.; Yangjin, D.; et al. Machine Learning Assists in the Design of Photocatalysts for Environmental Remediation: A Comprehensive Review. *Environmental and Microbial Technology* **2025**, *1*(1), 2.

Received: 16 October 2025
Revised: 14 November 2025
Accepted: 17 November 2025
Published: 22 November 2025

Abstract: Among various environmental remediation techniques, photocatalytic techniques, which uniquely take advantage of the sunlight, have attracted much attention. However, owing to the poor stability of catalysts, photocatalytic technology is predominantly confined to laboratory research at present, posing challenges for its large-scale application in environmental remediation and resulting in a scarcity of data on its full lifecycle management. This review proposes that machine learning (ML) may serve as a critical link in advancing photocatalytic technology from fundamental research to mature application processes. The data-explosive, scalable development approach facilitated by ML is expected to significantly overcome the limitations of the current trial-and-error method for developing photocatalysts. Integrated with a ML guided full life cycle assessment (LCA) encompassing "material design, process selection, material/energy consumption, pollution disposal, and environmental impact," this approach can contribute to forming a comprehensive photocatalytic environmental remediation technology system.

Keywords: machine learning; photocatalysis; environmental remediation; life cycle assessment

1. Introduction

With the continuous development of industrial production, environmental pollutants such as wastewater and exhaust gases have emerged accordingly [1,2]. The toxic and harmful pollutants contained therein, characterized by complex composition, resistance to degradation, bioaccumulation potential, and physiological toxicity, pose serious threats to human living environments and ecosystems [3–5]. Especially emerging contaminants (ECs), such as antibiotics, pesticides, and per-/polyfluoroalkyl substances (PFAS) can induce biological resistance, human diseases, and even mortality [6,7]. Volatile organic compounds (VOCs), when inhaled, may cause pulmonary diseases, carcinogenesis, and teratogenicity [8], while greenhouse gas emissions contribute to global climate change. Environmental media (water, air, soil) inevitably serve as sinks for these industrial metabolites, bearing the burden of all resources associated with human progress. Therefore, the adequate treatment of these environmental pollutants is a critical measure to mitigate environmental contamination, maintain ecological balance, and safeguard human health.

A wide range of technologies, including physical processes such as (1) adsorption, coagulation, and filtration, (2) biological techniques like phyto-stabilization, microbial metabolism and degradation, and constructed wetlands, and (3) chemical processes represented by advanced oxidation, have been extensively applied in environmental remediation [9–11]. These approaches address diverse environmental pollution issues, including industrial wastewater [12], municipal sewage [13], drinking water [14], watershed restoration, soil remediation [15], exhaust gas control, and atmospheric management. However, some of these

technologies suffer from one or more limitations, such as high operational costs, long treatment cycles, or the generation of secondary pollution [16,17]. Against the backdrop of China's dual carbon goals and the public's increasing demands for a better living environment, there is an urgent need to develop more novel, energy-saving, green, and efficient environmental remediation technologies. Photocatalytic technology has demonstrated broad application prospects in environmental pollution remediation [18]. It utilizes green and renewable solar energy to drive chemical reactions, enabling the degradation, transformation, and mineralization of specific environmental pollutants, thereby facilitating low-carbon and sustainable production. This technology has already played a significant role in remediating pollution across water, air, and soil media. Unlike conventional physical and biological remediation techniques, photocatalytic technology can convert or decompose pollutants into small molecules, eliminating their environmental hazards, and its reaction process is typically faster [19]. Furthermore, compared to other oxidation technologies, photocatalysis uniquely possesses both oxidation and reduction capabilities, allowing for the customization of redox processes based on the specific reaction system to maximize remediation efficiency [20]. Additionally, its reliance on clean and renewable sunlight as the energy input gives it inherent economic advantages. Nevertheless, the customized regulation of photocatalytic remediation systems, material selection, and product development still face numerous challenges, including unclear regulatory mechanisms [21], low efficiency in material screening, and difficulties in mass production and large-scale application. Therefore, it is essential to gain a comprehensive understanding of the reaction processes involved in photocatalytic environmental remediation, develop intelligent screening models for highly efficient candidate photocatalytic materials, and advance the practical application of photocatalytic technology.

Machine learning (ML) is an effective tool for processing large amounts of data and finding patterns from it, using data-driven methods to create models and solve key problems within them. ML techniques have already been successfully applied in many scientific fields, including functional materials, biology, catalysis, batteries and organic synthesis. In the field of photocatalysis, machine learning has been used for catalyst screening, design, and optimization, making it possible to identify efficient materials for specific reactions from a large number of semiconductor materials. By inputting specific descriptors and selecting valid data from the database, the efficiency of developing new photocatalysts has been unprecedentedly improved. Although existing studies have discussed ML for photocatalytic technology, including light harvesting, photogenerated charge separation, surface redox reaction and so on. The systematical investigation in environmental pollution remediation based on photocatalysis and the whole life cycle assessment by using ML method still remain knowledge gap.

This review aims to provide a novel perspective on understanding the integration of photocatalytic technology with ML in material design, optimization, synthesis, application scenario selection, and full life cycle management (LCA). It is noteworthy that the content under discussion diverges from the previous machine learning focus on the discovery and design of photocatalytic materials, instead emphasizing the progression from microscopic to macroscopic applications. Initially, summarized the current research status of machine learning, in photocatalyst design, synthesis, and reaction mechanism elucidation, with the goal of proposing a more efficient pathway for material development. Subsequently, presented research cases of photocatalytic technology in various aspects of environmental remediation (e.g., wastewater treatment, air purification, soil remediation) and analyzed their applicable conditions and existing challenges. Furthermore, to exam the pathways and significance of life cycle for photocatalytic technology, we discussed the combination of ML and LCA for its application potential and environmental management. Leveraging ML to precisely identify target photocatalysts from big data and accurately predict photocatalytic properties has emerged as a pivotal trend in advancing photocatalysis technology. Compared to the conventional trial-and-error approach, ML is expected to guide the rational design and discovery of novel catalysts with enhanced efficiency and balanced performance, thereby accelerating the practical implementation of photocatalytic technology.

2. Synthesis of Photocatalysts Based on Machine Learning

As the core of photocatalytic technology, photocatalytic materials have long faced prominent issues such as unclear structure-activity relationships [22,23], complex preparation and modulation [24], and insufficient activity and stability [25], which greatly limit their application and development. By leveraging large-scale machine learning models and big data analytics to predict the functional properties of different structures of photocatalytic materials and tailoring material compositions based on desired properties, the success rate of material preparation can be significantly enhanced while reducing trial-and-error costs [26].

The data preprocessing stage of machine learning mainly includes core steps such as data cleaning, missing value processing, normalization/normalization, and feature selection. Firstly, duplicate data and outliers should be

eliminated. Subsequently, check the missing values and take actions to fill or delete them based on the reasons for the missing and the distribution of the data. Next, the obtained data will be normalized, and nonlinear transformation can be used to improve the distribution shape of the data. Finally, in order to enhance the credibility of the model, multi factor simulation should be adopted for photocatalyst screening and process optimization. At the same time, appropriate experimental verification will further improve the reliability of the data.

2.1. High-Throughput Screening of Photocatalysts

Machine learning, a branch of artificial intelligence that relies on algorithms and statistical models to discover target catalyst structures and make predictions from large datasets, has been employed to accelerate materials development [26–28]. Compared to traditional trial-and-error approaches for preparing photocatalytic materials, ML significantly enhances the screening efficiency for new materials [29,30]. It can also inversely generate material structures based on user-defined performance requirements, thereby guiding material synthesis. The key challenge facing materials informatics is to obtain sufficient and reliable material data. The dataset must contain input variables that are clearly defined by the model (such as the microstructure, properties, or synthesis conditions of the material) and the macroscopic properties of interest predicted by the model training. The fundamental steps for constructing an ML model include: collecting data to form a training dataset, generating and selecting relevant mathematical descriptors that encode material properties, choosing appropriate algorithms and building the model, and evaluating the model's quality and predictive power [31]. Although ML has been used for photocatalyst design, reaction dynamic prediction, there are still few reports on machine learning models used to explain the electron transfer mechanism in photocatalytic systems, which may be due to the lack of in situ techniques to obtain sufficient data.

The design of novel photocatalysts via machine learning primarily depends on crystallographic data of the photocatalyst itself, such as phase structure and microstructure. Three methods can be employed to acquire such data: (1) searching existing databases to obtain relevant data; (2) collecting data under various environmental parameters from literature; and (3) conducting related experiments to obtain corresponding experimental data. Figure 1 shows the flowchart of the intelligent algorithm for predicting the photocatalytic performance of photocatalysts [32].

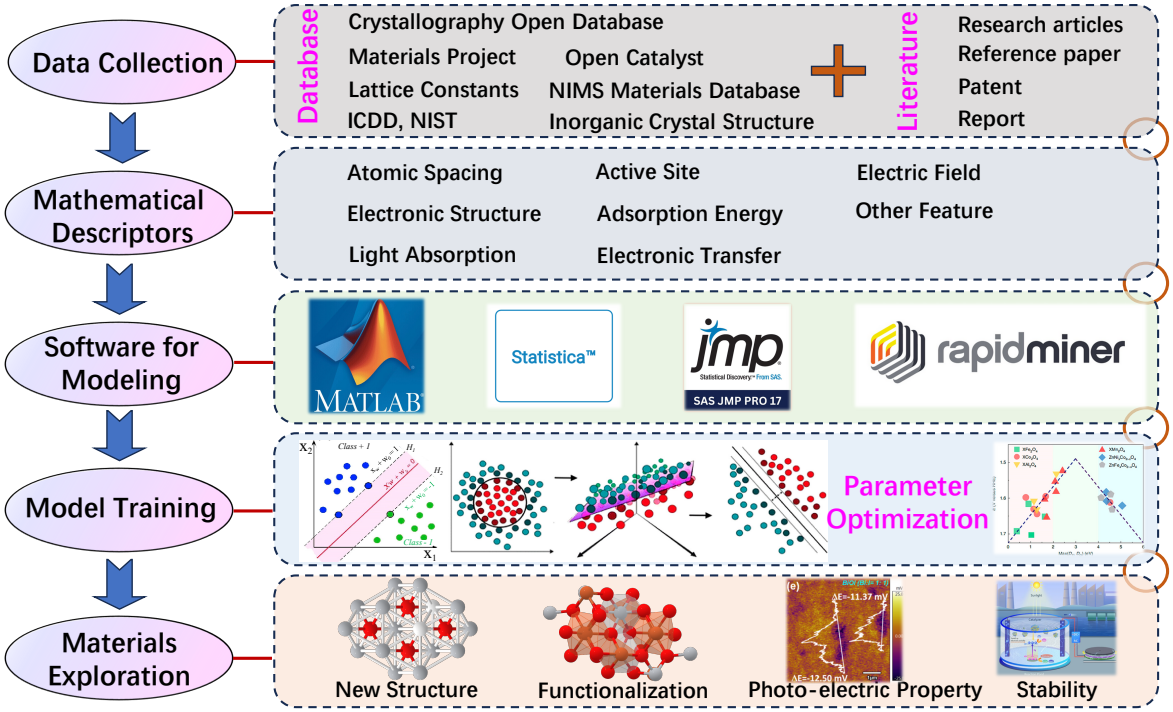

Figure 1. Procedures of AI for the selection and prediction of photocatalysts.

Through screening a vast photocatalyst database for specific functional catalysts, selected descriptors were employed to encode the structural characteristics of the photocatalysts. For instance, Soo Han Sen et al. [33] utilized a machine learning approach to discover a novel lead-free metal halide perovskite photocatalyst for the aerobic oxidation of styrene. This catalyst achieved an 80% yield in converting styrene to benzoic acid,

representing a 13-fold performance enhancement over $Cs_2AgBiBr_6$. Specifically, multiple rounds of iterative machine learning models were applied to screen 18 metal halide perovskites. ML parameters were constructed based on the fundamental chemical structure unit of perovskites (ABX_3) and correlated with benzoic acid yield. Further hyperparameter tuning was performed using Bayesian optimization via the Scikit-Optimize package, and leave-one-out cross-validation (LOOCV) was employed to individually predict the yield for each benzoic acid sample. After evaluating common ML algorithms such as linear regression, gradient boosting, random forest, and neural networks, the neural network algorithm was ultimately selected due to its highest LOOCV prediction accuracy, achieving an R^2 score exceeding 0.96, which demonstrated the reliability of the ML predictions. Through a series of A-/B-site substitutions and electronegativity analyses, it was found that $BA_2CsAg_{0.95}Na_{0.05}BiBr_7$ (where BA denotes n-butylammonium) as the primary A-site component exhibited a remarkable yield of 80%. The study highlights that continued multi-dimensional ML analysis can theoretically enable rapid screening of chemical structural information for catalysts with specific properties, thereby guiding material synthesis. However, using different ML methods to screen or predict photocatalytic materials and their property parameters, there is often a bias in the predicted results [31]. For example, regression methods are more advantageous when the dataset size is small or when it is necessary to clarify the linear/nonlinear relationship between features and target variables. In complex tasks such as photocatalytic hydrogen production rate and pollutant degradation efficiency, neural networks are usually more accurate than traditional regression methods. The applicability comparison of different methods is shown in Table 1.

Table 1. Comparison of advantages and limitations of various ML methods.

ML Methods	Applicable Scenarios	Advantages	Limitations
Regression	Small data volume, clear relationship between features and targets	High computational efficiency, strong interpretability of the model, suitable for quickly screening key parameters	Limited ability to model complex non-linear relationships
Gradient boosting	Medium scale data, balancing accuracy and computational cost	Improving prediction accuracy through ensemble learning, with strong robustness to outliers	Hyperparameter tuning is complex and may result in overfitting, leading to longer training times
Neural networks	Large scale data, high-dimensional features	Automatic feature extraction, strong modeling ability for complex nonlinear relationships, suitable for multi task learning	Requires a large amount of annotated data, high training costs, and poor model interpretability
Random forest	There is a lot of data noise and quick verification is required	Strong anti overfitting ability, capable of handling high-dimensional features, and providing feature importance analysis	Sensitive to hyperparameters, prediction results may be unstable

In the preparation of photocatalytic materials, elemental doping serves as a crucial strategy for modulating their photo responsive properties, band structures, and electronic states [34–36]. Conventional methods often involve large-scale doping trials with various elements to identify optimal performance, which suffers from high experimental burden, significant errors, and low efficiency [37]. In response to these challenges, Zwijnenburg et al. [38] employed a Gaussian Process Regression (GBR) model to screen 6354 conjugated copolymers for discovering novel photocatalysts with high sacrificial hydrogen evolution rates. Each copolymer was encoded using four descriptors: electron affinity, ionization potential, optical band gap, and light transmittance. Through iterative ML, it was found that high hydrogen evolution activity requires a combination of negative electron affinity, large positive ionization energy, wide band gap, and good solvent dispersibility-thereby enabling rapid identification of the physicochemical characteristics of target catalysts. ML can integrate empirical models with predictive analytics to evaluate the properties of catalysts after elemental doping, allowing efficient screening of doping strategies-including dopant type, concentration, and heteroatom ratio-tailored for specific reactions. In summary, machine learning is transforming conventional approaches to the discovery, screening, and performance prediction of photocatalysts, enabling theoretically guided selection of materials for diverse photocatalytic applications.

2.2. Analysis of Active Sites and Mechanism

The solar-driven water splitting reaction utilizing photocatalytic materials represents one of the most critical energy conversion processes for green hydrogen production. However, the facile recombination of photogenerated electron-hole pair remains a major factor limiting photocatalytic activity [39,40]. Elemental doping can readily modulate the semiconductor properties of host materials, thereby optimizing electron-hole separation efficiency. As

primary functional sites for regulating the activity of photocatalysts, dopant elements exhibit highly complex combinatorial patterns and property influences, making trial-and-error-based material exploration extremely time-consuming. Machine learning and deep learning (DL, is a specialized subset of ML that uses artificial neural networks (ANNs) with multiple layers (deep architectures) to model complex patterns in data) techniques offer promising solutions to this challenge. Wang et al. [41] employed ML to predict the photocurrent density of single-element-doped hematite photoanodes and discussed the key characteristics of dopants (Figure 2a). They defined two target variables, j_{NaOH} and j_{H2O2} (where j_{NaOH} was measured under standard assessment conditions in an aqueous 1 M NaOH solution without any sacrificial reagent, and j_{H2O2} was measured under identical conditions with H_2O_2 as the sacrificial agent), and found that the j_{H2O2} prediction model achieved high accuracy by reducing the consideration of surface charge recombination and water oxidation kinetics. Tachikawa et al. [42] developed a highly reproducible synthesis protocol for multi-element-doped hematite photoanodes incorporating two or three dopant elements, testing a total of 39 dopant elements and synthesizing 97 unique sample compositions (Figure 2b).

Subsequently, an ML regression model was constructed to interpret the hematite dataset. Elemental features and analytical data were used as explanatory variables, while the photocurrent density J ($mA \cdot cm^{-2}$) at 1.6 V vs. RHE ($J_{1.6V}$) was set as the target variable. Furthermore, extrapolative predictions were performed for virtual hematite samples. Although the variation in the photoelectrochemical (PEC) performance of multi-element-doped hematite photoanodes arises from complex interactions among each element in the samples, the extrapolation predictions readily captured doping induced or compositional trends. These findings highlight the effectiveness of ML in accelerating the design of heterogeneous photocatalysts and provide strategic insights for developing efficient solar energy conversion systems in future studies. Table 2 lists some comparisons when design and screen photocatalysts from using different models or input various parameters. The use of different ML models and input descriptors can influence the performance prediction outcomes of photocatalysts. Therefore, during the photocatalyst screening phase, a comprehensive comparison should be conducted to select the most suitable prediction model.

Table 2. Comparison of different ML models for photocatalyst prediction.

Models	Input Parameters	Outcomes	References
Neural networks	Percentage of A_m, B_n, and X_o in ABX_3, crystal space group, yield of benzoic acid	yield of benzoic acid	[33]
Regression and classification	Radius, Formation energy, Stability, Volume per atom, Vacancy energy	band edge positions, band gap types	[43]
Polynomial regression	Time, pH, photocatalysts, dosage, process, pollutants, concentration	R^2: 0.928; MAE:6.01; RMSE: 9.17	[44]
Support Vector Regression		R^2: 0.94; MAE:4.07; RMSE: 8.31	
XGBoost		R^2: 0.958; MAE:2.61; RMSE: 6.85	
Random Forest		R^2: 0.965; MAE:2.83; RMSE: 6.29	
Gradient Boosting		R^2: 0.96; MAE:5.81; RMSE: 6.74	
Neural networks		R^2: 0.97; MAE:2.7; RMSE: 5.88	
Gradient boosted regression	charge mobility, light harvesting	optimal Al dopant amount	[45]

In photocatalytic technology applications, catalyst deactivation often occurs when pollutants adsorb extensively on the catalyst surface or active sites [46–48]. The reaction mechanisms are highly variable, making it challenging to identify a universal method to suppress catalyst deactivation. Machine learning can assist in analyzing pollutant reaction mechanisms by predicting the reaction processes and outcomes in catalytic systems, thereby enabling proactive solutions. Researchers [49] employed computational methods to predict the adsorption behaviors of small molecular acids, such as tryptophan, coniferyl alcohol, succinic acid, gallic acid, and trimestic acid on TiO_2 surfaces, along with their inhibitory effects on the degradation of p-chlorobenzoic acid (Figure 2c). The study established a ranking of the contribution of these inhibitors. Furthermore, density functional theory (DFT) and machine-learned interatomic potentials (MLIPs) were used to investigate these interactions. It was found that the spatial arrangement of molecular functional groups and electronic interactions significantly influence adsorption kinetics and corresponding inhibitory behavior, which greatly aids in analyzing photocatalytic

reaction mechanisms. In the photocatalytic degradation of lignin to produce high-value chemicals, enhancing catalytic activity and selectivity under mild conditions has long been a challenge. By applying machine learning methods and comparing different training models, it was discovered that the dissociation energy of bond cleavage increases with the number of methoxy groups attached to the benzene ring. The study also revealed that reaction conditions contribute 39.22% to the feature importance of the model, and oxygen is a crucial atmospheric component in the photocatalytic degradation of lignin. These findings underscore the significant role of machine learning in elucidating reaction mechanisms.

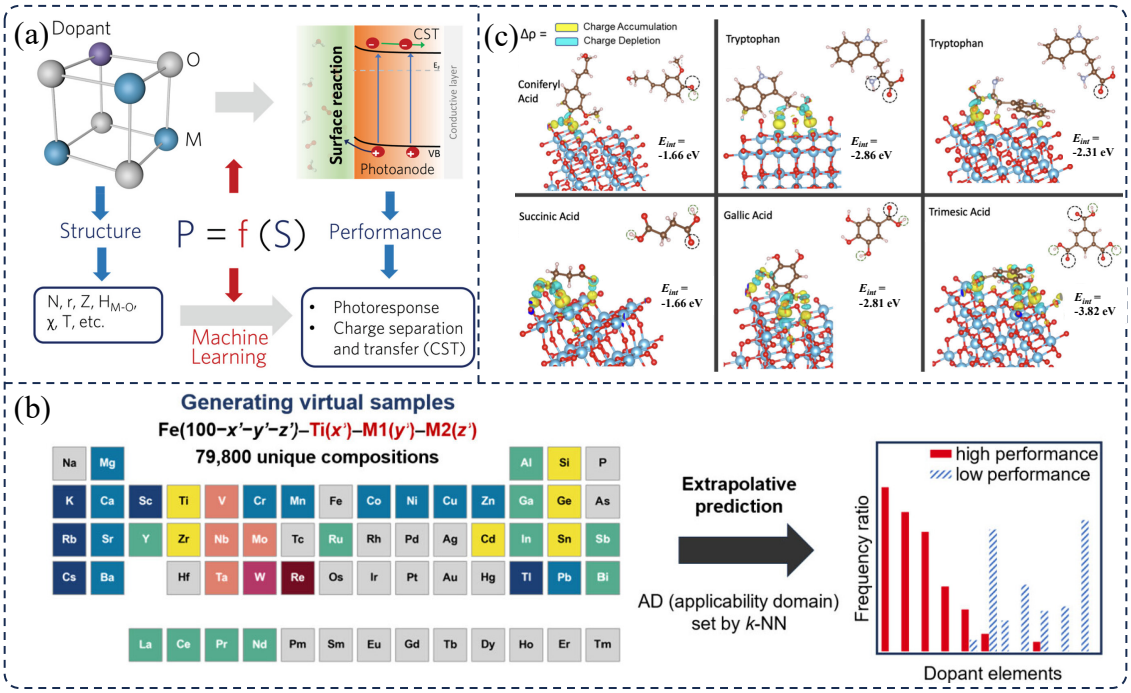

Figure 2. Machine learning in optimization of active sites. (**a**) Schematic diagram of structure optimization. Reproduced with permission [41]. Copyright 2022, by Wiley-VCH. (**b**) Performance prediction of dopant elements in photocatalyst, Reproduced with permission [42]. Copyright 2025, American Chemical Society. and (**c**) prediction of molecule dynamics on photocatalyst surface. Reproduced with permission [49]. Copyright 2024, American Chemical Society.

2.3. Optimization of Catalytic Performance

The conventional preparation of photocatalysts requires adjusting multiple parameters, including catalyst type, combination methods, preparation temperature, time, and loading amount, to obtain materials with relatively satisfactory performance [50,51]. This manual optimization process is challenging to execute, time-consuming, and suffers from poor reproducibility, making it difficult to meet the demands of diverse catalyst development. In light of this, Professor Gong Jinlong's research team [52] at Tianjin University proposed a machine learning-based prediction model for catalyst performance optimization, which successfully decouples the atomic properties (A), reactant effects (R), synergy (S), and coordination effects (C) of dual-atom sites (Figure 3a). Driven by the ARSC framework, researchers can rapidly identify optimal catalysts for various products without performing over 50,000 density functional theory calculations. Experiments confirmed that Co-Co/Ir-Qv3 is the optimal bifunctional oxygen reduction and evolution electrocatalyst. The ARSC model framework comprises four key components: (i) an original descriptor (φ_{xx}) for atomic property effects via d-band shape analysis; (ii) a screening principle (φ_{opt}) for potentially ideal heteronuclear dual-atom catalysts based on reactant effects; (iii) a machine learning-based descriptor (φ_{xy}) for synergy effects, achieved through feature engineering and feature selection/sparsification algorithms grounded in the physical meaning of φ_{xx}; and (iv) a final universal descriptor model (Φ) incorporating coordination effect quantification and experimental validation. This study provides valuable insights for the design and optimization of photocatalysts.

Solar photoelectrochemical (PEC) water splitting is an efficient method for converting solar energy into hydrogen energy, representing a promising approach for renewable energy production [53,54]. However, the efficiency of PEC reactions remains relatively low due to the properties and defects of electrodes, necessitating the use of suitable co-catalysts for assistance [55]. The PEC system, composed of an electrolytic cell, photoelectrodes, and co-catalysts, is highly complex with numerous parameters, making system optimization costly. To address this,

Zhu et al. [56] employed machine learning to optimize a $BiVO_4$ photoanode system. They compiled a dataset of 112 experimental data points on $BiVO_4$ photoanode-catalyzed water splitting from 84 literature sources. By comparing neural network models, Random Forest, Bagging, AdaBoost, and Gradient Boosting models, they found that the Random Forest model exhibited the best generalization capability, with a test accuracy of 70.37% and an AUC of 0.784. Furthermore, optimization of conditions such as co-catalyst thickness, photoanode thickness, and electrolyte concentration identified the optimal reaction parameters. Lu et al. developed a NN model to leverage DFT calculations, and studied the adsorption energy of OH* on IrPdPtRhRu with random element distributions and 12 unique coordination environments (Figure 3b). In the future, machine learning will continue to advance in multi-objective optimization balancing, including photocatalyst cost screening, performance optimization, and durability design, guiding photocatalyst design from traditional trial-and-error methods toward high-efficiency prediction and promoting the practical application of photocatalytic technology.

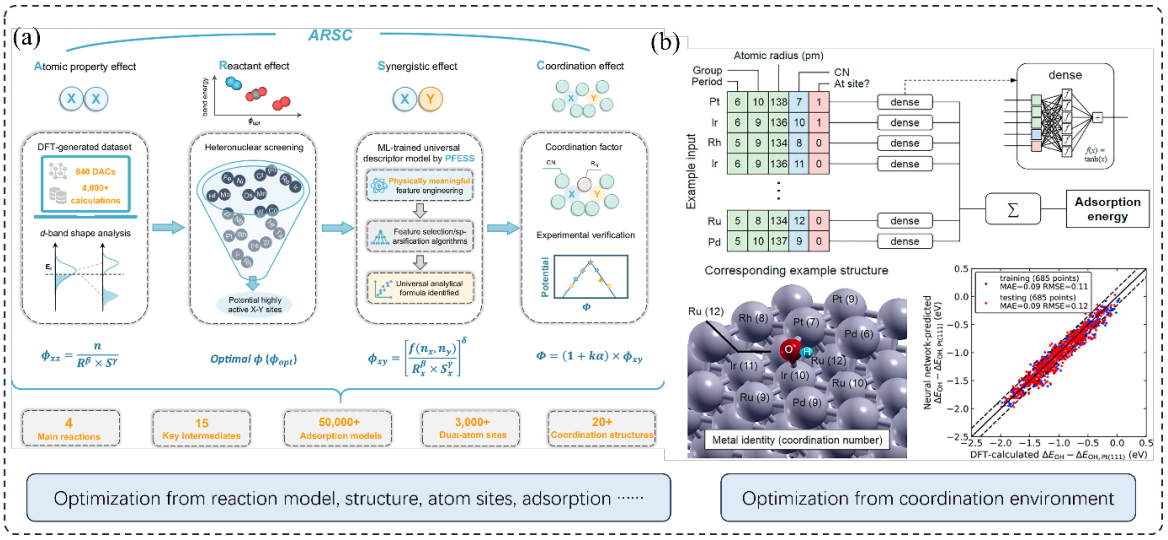

Figure 3. (**a**) Optimization procedure of photocatalyst by using ML method from atomic property effect, reactant effect, synergistic effect and coordination effect aspects. Reproduced with permission [52]. Copyright 2024, by Springer Nature. (**b**) optimization of ML model though various systems. Reproduced with permission [31]. Copyright 2022, by ACS Publications.

3. Advanced Application of Photocatalysts in the Remediation of Environmental Pollutants

3.1. Reaction Process of Photocatalytic Technology in Environment Remediation

Photocatalytic reactions have existed since the beginning of life evolution on Earth. The most widespread photocatalytic process originates from the photosynthesis of marine microalgae and plants, where light energy acts as a medium to drive a series of biochemical reactions that convert carbon dioxide into stored organic matter. Photocatalytic technology has been extensively studied and improved for applications in environmental water remediation, atmospheric purification, and industrial pollutant degradation. Semiconductor-based photocatalysis harnesses solar energy to initiate reactions. As illustrated in Figure 4, when the absorbed energy is sufficient to disrupt the stable state of ground-state electrons, electrons are excited from the valence band (VB) to the conduction band (CB), generating free electrons and holes, accompanied by the production of quasiparticles such as excitons and phonons [57]. These quasiparticles undergo a series of physical and chemical processes within an extremely short period, eventually being annihilated within the material matrix as vibrations or heat [58]. Most of the photogenerated electrons and holes tend to rapidly recombine and dissipate in the form of vibration or heat. Only a small fraction of the photogenerated electrons migrate to the material surface and interact with the surrounding medium, triggering chemical reactions [59]. Simultaneously, an equal number of photogenerated holes remain in the valence band, these exhibit strong oxidation potential and tend to extract electrons from external species to reach equilibrium. The regions near the valence and conduction bands of photocatalytic materials thus become critical sites for energy exchange and chemical reactions. In environmental remediation, photocatalysis primarily degrades, transforms, or mineralizes pollutants through interfacial mass and energy exchange, commonly occurring at solid-liquid, gas-liquid, and gas-solid interfaces [60,61]. However, two major technical challenges remain: first, a significant portion of the photogenerated charge carriers recombine within the material bulk before reaching the surface, resulting in low charge separation efficiency; Second, the lifetimes of

reactive species (e.g., electrons and holes) that reach the surface are extremely short, and their concentrations further decrease during diffusion [62]. Enhancing interfacial interactions is crucial for improving the utilization efficiency of these active species.

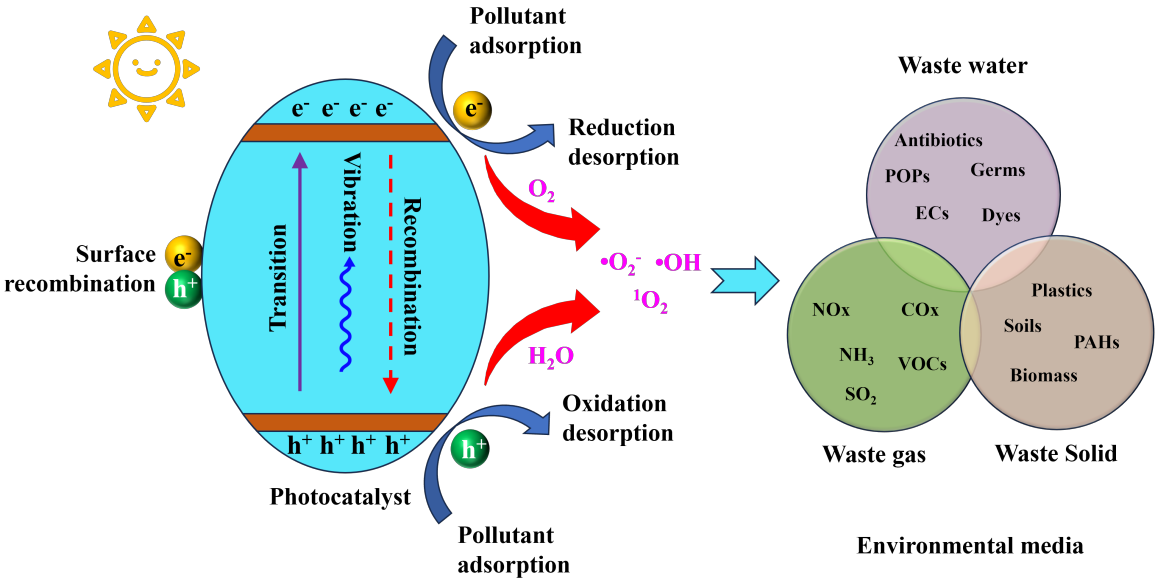

Figure 4. Photocatalytic reaction process between photocatalysts, molecules and environmental pollutants.

3.2. Interfacial Interaction Enhanced Photocatalysis Process

The advantage of machine learning is that it can empower catalysts during the catalyst screening and synthesis stages based on the scenario of photocatalytic reactions. For example, in gas-solid reaction systems, optimizing catalyst performance using machine learning should be predicted based on descriptors such as adsorption energy, band structure, light absorption, and mass transfer efficiency. In solid-liquid systems, in addition to considering the photogenerated charge separation and redox ability of the catalyst itself, the hydrophilicity of the photocatalyst and its ability to adsorb pollutants should also be optimized to enhance its application performance (Figure 5). The design, screening, and optimization of photocatalysts have been discussed in the second part. This section mainly discusses the typical application scenarios of photocatalytic technology, thus connecting the discussion of machine learning from material development to full lifecycle assessment.

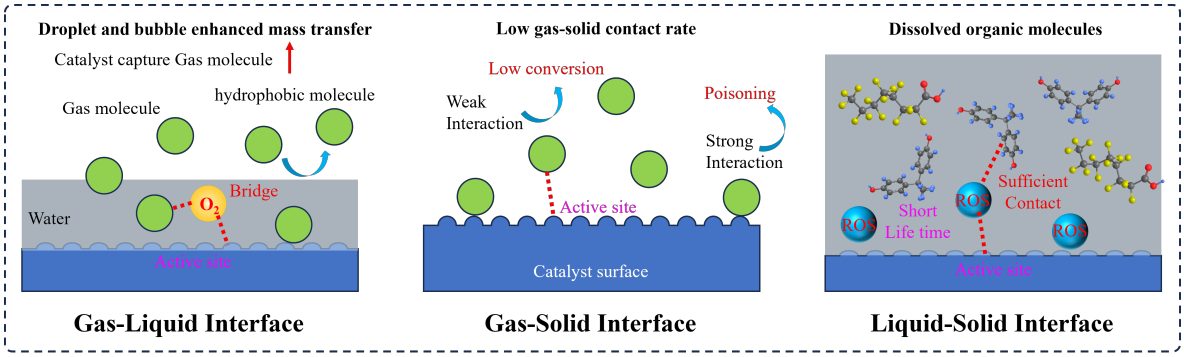

Figure 5. Interfacial interaction in photocatalysis between gas, solid and liquid multi-phase systems.

In photocatalytic reactions such as CO_2 conversion, VOCs degradation, and nitrogen oxide transformation, photocatalytic activity primarily relies on gas-solid interfacial processes [63]. These interfacial reactions are governed by the interactions between gas molecules and the catalyst. Under weak interactions, insufficient contact between the gas and solid phases results in low pollutant conversion rates [64]. Conversely, under strong interactions, degraded pollutant molecules struggle to desorb from the catalyst surface, leading to occupied active sites and catalyst poisoning [65,66]. Meanwhile, in gas-liquid-solid reaction systems, regulating the concentration of active species at the solid-liquid interface via gaseous media (e.g., oxygen) can enhance the mass transfer of reactive substances and the diffusion of pollutants. Therefore, precisely manipulating the gas-liquid-solid

interfacial reaction processes is crucial for improving photocatalytic performance. Wang et al. [67] developed a novel three-phase photocatalytic microreactor that enhances the degradation of dyes in wastewater by generating periodic bubbles within the microfluidic flow. In this process, the bubbles serve three essential functions: (1) Oxygen molecules act as transport mediators for photocatalytic active species, facilitating the degradation of target pollutants; (2) They intensify mass transfer efficiency between the solid catalyst and liquid pollutants at the solid-liquid interface, ensuring efficient contact between pollutant molecules and active species; (3) The hydraulic disturbances induced by oxygen bubbles help remove carbon deposits from the catalyst surface and suppress catalyst agglomeration, thereby refreshing the solid-phase interface. This synergistic gas-liquid-solid interaction significantly improves the efficiency of photocatalytic water treatment.

Solar-driven interfacial water evaporation (SDIWE) is an emerging technology for clean water production powered by abundant solar energy [68–70]. However, its application is hindered by the issue of volatile organic compounds (VOCs) escaping into the condensate. To address this, Fan and his team [71] constructed a photocatalytic-Fenton coupled gas-liquid-solid reaction system. They employed a nanofiber membrane prepared with photocatalysts as the solar evaporator, which simultaneously enables in situ generation of H_2O_2 during evaporation. The H_2O_2 is subsequently activated by Fe^{2+} to produce reactive radicals. VOCs released during evaporation are rapidly degraded upon contact with these active species, ensuring efficient decomposition during fast vapor generation. This multi-phase reaction system enhanced VOCs removal efficiency by sixfold and prevented environmental release of VOCs. Oxygen serves as a natural and highly efficient electron scavenger. Its reaction with photogenerated electrons produces highly reactive superoxide radicals. However, the low solubility and slow mass transfer rate of oxygen in water, particularly in wastewater, severely restrict its electron-scavenging capability, thereby considerably limiting the efficiency of photocatalytic reactions. Inspired by biomimetic superhydrophobic materials. Feng et al. [72] constructed a gas-liquid-solid triple-phase photocatalytic reaction system. The superhydrophobic surface can form air pockets connected to the atmosphere when in contact with liquid, thereby introducing a gas phase to the reaction interface. They deposited semiconductor catalysts on a superhydrophobic substrate. This composite structure allows water to submerge the catalyst particles while leaving the substrate unwetted, thus forming a reaction interface where gas, liquid, and solid phases coexist. Oxygen can be rapidly transported from the air to the reaction interface, a process that is five orders of magnitude faster than diffusion through water. As a result, a high local oxygen concentration is maintained at the reaction site, which effectively promotes the separation of photogenerated electrons and holes and significantly enhances the reaction kinetics. Compared to conventional liquid-solid two-phase systems, the triple-phase system exhibits markedly improved quantum efficiency and reduced charge recombination, enabling the photocatalytic reaction to maintain high quantum yield even under relatively high light intensities (up to 8 times that tolerated in two-phase systems).

In photocatalytic air purification, CO_2 conversion, automotive exhaust purification, and industrial flue gas treatment, catalytic degradation and transformation primarily occur at the gas-solid interface [73]. The physical and chemical processes involved in photocatalytic air purification are highly complex as a heterogeneous catalytic system. The reaction of gaseous reactants on the surface of solid photocatalysts can be divided into several steps, generally including diffusion of gaseous pollutants to the solid surface, adsorption of pollutants, surface chemical reactions, and desorption and diffusion of products back into the gas phase [74]. Optimizing the mass transfer efficiency and adsorption behavior of target waste gases in multi-component gas mixtures on the catalyst surface can effectively enhance the photocatalytic reaction efficiency. Based on this, Ye et al. [75] developed a photo-Fenton reaction system using an alkalized Fe^{3+} doped carbon nitride photocatalyst. This system can generate a considerable abundance of oxygen-related radicals that participate in the photocatalytic reaction. Unlike traditional Fenton reactions in aqueous media, an alkaline rather than acidic surface provides a suitable chemical environment for this solid-gas interface Fenton process. The photocatalytic system exhibited highly efficient and versatile activity for the photodegradation of volatile organic compounds (VOCs). In particular, the photodegradation rate of isopropanol with this system achieved an amplification factor of 270 compared with pristine g-C_3N_4, corresponding to a high apparent quantum yield of approximately 49% at 420 nm.

The adsorption and capture of gases depend on the adsorption capacity and selectivity of the photocatalyst, where gases can be trapped in the pores via van der Waals forces (physisorption) or through chemical bonds formed between the photocatalyst and the adsorbate (chemisorption). To enhance chemisorption capacity, it is often necessary to create specific adsorption sites on the photocatalyst, including surface functionalization [76,77], surface atom coordination, and modulation of electron density (electron-deficient or electron-rich regions). In Dong's work, a combination of temperature-programmed desorption (TPD) and density functional theory (DFT) calculations was employed to elucidate the effect of Ba vacancy engineering on reactant adsorption. The formation of Ba vacancies in $BaSO_4$ was initially indicated by X-ray Absorption Fine Structure (XAFS) spectroscopy and DFT. TPD experiments confirmed that $BaSO_4$ with Ba vacancies (BSO) adsorbed more NO_4 compared to pure

$BaSO_4$ (PBSO). Xie and colleagues investigated the adsorption mechanism of gaseous acetaldehyde and o-xylene on rGO-TiO_2. When the specific surface area of pure TiO_2 and rGO-TiO_2 materials showed no significant difference, the saturated adsorption of acetaldehyde and o-xylene increased with higher rGO content, indicating that chemical functional groups play a crucial role in the adsorption process.

In practical applications, Oriol Roig et al. [78] demonstrated an openable double-skin façade assembly with a cavity incorporating a series of slats that filter and purify air through photocatalytic reactions (TiO_2). This assembly integrates ventilation, shading, and air purification functions. The photocatalytic elements are applied as a coating on the exposed surfaces of the slats. This coating interacts with oxidant compounds such as oxygen (O_2) present in the air and is activated by ultraviolet solar radiation. Titanium dioxide (TiO_2) is the most widely used photocatalytic element in this reaction. The photocatalytic effectiveness of three types of photocatalytic coatings was tested on five substrate materials: extruded aluminum (AX), single-side perforated printed ceramic (Cl-1C), double-side perforated printed ceramic (Cl-2C), extruded ceramic (CX), and medium-porosity aluminum foam (AE-M). Laboratory results on air purification indicated that specific samples achieved a reduction of air pollutants by up to 9% degradation for NO and NO_x.

In a field study in Baton Rouge, Louisiana [79], photocatalytic asphalt pavement was employed to investigate the purification performance of vehicle exhaust. A Davis 6152 Wireless Vantage Pro weather station was installed on-site to continuously record and store meteorological data-including humidity, ambient temperature, wind speed, and solar radiation-at one-minute intervals. Under suitable conditions, the removal rate of NO_x reached 60% within 5 min. Increased traffic flow led to higher NOx concentrations due to additional pollutant emissions, which in turn resulted in a decrease in the removal rate. As ambient humidity increased, excessive water vapor accumulated on the TiO_2 surface, inhibiting contact between NOx and the catalyst and causing a significant decline in removal efficiency. Under simulated maximum wind speed conditions (4 m/s), the photocatalytic degradation efficiency of NOx decreased to 42%, owing to reduced contact time between pollutants and the catalytic surface.

Furthermore, optimizing the local microenvironment at the gas-solid interface can significantly enhance reaction selectivity and efficiency. For instance, Li et al. [80] constructed an NH_2-MXene/TiO_2/NH_2-MIL-125 (Ti-NMT) hierarchical interface system. This system utilizes the metallic conductivity of MXene to accelerate electron transport, while the Lewis acid-base interaction of amine groups enhances CO_2 adsorption. Simultaneously, the synergy between an S-scheme heterojunction and a Schottky barrier promotes charge separation. The localized surface plasmon resonance (LSPR) effect of MXene not only increases hot carrier density but also significantly reduces the activation energy of the catalytic reaction, achieving 100% selective conversion of CO_2 to CO in industrial flue gas. Through heterointerface engineering and functional group optimization, this system has successfully overcome technical bottlenecks in the resource recovery of CO_2 from industrial exhaust gases.

Photocatalysts have been extensively investigated for the degradation of organic pollutants in water bodies, such as antibiotics and antibiotic resistance genes in pharmaceutical wastewater, phenolic compounds, fluorinated pollutants, and other toxic organic contaminants in industrial wastewater [81,82]. The degradation performance of photocatalytic materials primarily depends on the collision probability and adsorption behavior between the catalyst interface and water molecules or dissolved pollutant molecules, as well as the generation of primary active species. Enhancing the synergistic effects at the solid-liquid interface is a crucial strategy for improving degradation efficiency. Dong et al. [83] developed a photocatalytic system based on halloysite nanotube-supported molybdenum disulfide and iron oxyhydroxide. Benefiting from the hydrophilicity and surface charge characteristics of halloysite, molybdenum disulfide was uniformly dispersed in water, thereby enhancing solid-liquid contact. Meanwhile, halloysite exhibits a strong affinity for positively charged organic molecules or functional groups, increasing the probability of contact between pollutants and the catalyst surface in aquatic environments. Constructing a thin passivation layer on the semiconductor surface can effectively suppress non-radiative recombination of photogenerated carriers caused by surface states. As reviewed by Zheng's group [84], such a passivation layer not only reduces surface defects but also modulates the band structure of the semiconductor, increasing the photovoltage (thermodynamic driving force) and promoting interfacial charge transfer kinetics. Suitable passivation layers (e.g., thin metal oxide layers like TiO_2 or Al_2O_3) form an energy gradient between the semiconductor and the liquid interface, effectively guiding the directional migration of photogenerated electrons or holes to the interface for redox reactions.

Furthermore, the mass transfer efficiency of reactants and products at the solid-liquid interface represents another rate-limiting step in photocatalytic reactions. By modulating the surface wettability of catalysts, the interfacial mass transfer process can be optimized, thereby enhancing reaction efficiency. Innovatively, researcher [85] constructed a superhydrophilic [86]/superhydrophobic composite photocatalyst (OCUN/T) for efficient degradation of methanethiol (CH_3SH). The hydrophilic TiO_2 nanoparticles facilitate water molecule adsorption and hole-driven generation of •OH, while the octadecylphosphonic acid (OPA)-modified Cu-doped UiO-66-NH_2 (OCUN) exhibits

superhydrophobicity (contact angle: 152.12°), promoting oxygen adsorption and electron-driven formation of $\bullet O_2^-$. This dual-domain synergistic effect enables the composite to simultaneously generate two primary reactive species (•OH and $\bullet O_2^-$) at the gas-liquid-solid triple-phase interface, achieving highly efficient degradation of CH_3SH while suppressing secondary pollution. In a separate study, Yao et al. [87] investigated the influence of hydrogen-bond networks in water-methanol mixed solvents on the reaction rate of photocatalytic methanol reforming. With increasing molar ratio of methanol, the product yield and cluster diffusion rate exhibited a remarkable V-shaped variation pattern, reaching a minimum near the water-methanol ratio of 7:1 (W7M1). This reveals that the synergistic diffusion of solvent-solute clusters is one of the kinetic-determining steps in solid-liquid photocatalytic reactions: the strength of the hydrogen-bond network directly affects the diffusion rate of molecular clusters to the catalyst surface, consequently influencing the adsorption and cleavage rates at surface active sites. This work provides the first in situ evidence of the impact of hydrogen-bond networks on photocatalytic efficiency, highlighting the importance of regulating interfacial solvation structures.

3.3. Photocatalysis Cooperation with Multi-Media Enhancement for Environmental Pollution Remediation

Photocatalysis-Photosynthetic microorganism-Plant Remediation. In the field of soil site remediation, photocatalytic technology has been practically applied in synergy with plants, microorganisms, permeable reactive barriers (PRBs), and other systems to overcome the limitations of single technologies in simultaneously removing, degrading, and mineralizing organic pollutants [88]. Photosynthetic microorganisms have been experimentally demonstrated to degrade pollutants such as microplastics in soil or water through metabolic processes (Figure 6). Due to the high surface area in aquatic environments, sunlight availability, and abundant nitrogen and phosphorus, plastic debris provides an excellent growth substrate for microalgae [89]. The capabilities of microalgae and cyanobacteria may prove more advantageous and sustainable, as they eliminate the need for externally added cofactors. As hosts for photo-biocatalytic reactions, the development of recombinant cyanobacterial and microalgal applications could contribute to plastic pollution remediation by expressing selected enzymes capable of degrading these polymers while utilizing light. This is particularly feasible when using engineered strains through genetic modification or evolutionary adaptation, where nanoparticles (NPs) can be considered substrates for photo-biocatalytic reactions [90]. Photocatalytic degradation combined with phyto-stabilization technology has been successfully applied at a former chemical plant in New Jersey, USA. A combined system of "photocatalytic PRB + poplar remediation" was used to treat contaminated soil. Within five years, the trichloroethylene concentration in the soil decreased from 580 mg/L to 0.05 mg/L. In this system, the PRB process served as the primary functional unit for removing soil contaminants, while pollutants near the surface and at deeper layers were gradually broken down through photocatalytic oxidation and plant metabolism, respectively, achieving highly efficient remediation.

Physical Field Enhanced Photocatalysis performance. Studies have demonstrated that physical field assistance can enhance photocatalytic activity from the perspectives of kinetics, thermodynamics, and reaction pathways, such as ultrasonic fields, thermal fields, electric fields, and gravitational fields [91–93] (Figure 6). Although the synergistic effects between these physical fields and photocatalysts differ, each possesses its own distinct advantages.

The combination of ultrasound and photocatalysis is widely employed in various applications, including aqueous pollutant degradation [94], plastic conversion [95], hydrogen production [96], and in-situ synthesis of hydrogen peroxide [97,98]. Under ultrasonic irradiation, materials exhibit a piezoelectric effect that promotes bulk electron separation, effectively addressing the issue of low charge carrier separation efficiency in photocatalytic materials. Lu et al. [99] developed a ternary hybrid dual S-scheme heterojunction material based on $MoS_2/FeS_2@FeMoO_4$ with a hollow sea-urchin-like morphology. In this structure, MoS_2 possesses a certain piezoelectric effect and excellent photocatalytic performance, while the introduction of the FeS_2 phase enhances the material's absorption and response to visible light. This system enables the generation of hydrogen peroxide under ultrasonic-light conditions, followed by its in-situ activation. Owing to the synergistic effects of the heterogeneous interpenetrating structure, piezoelectric response, and light irradiation, the catalytic activity is significantly enhanced. The piezo-photocatalytic conditions demonstrated the highest plastic degradation rate-after 30 h of reaction, the degradation rate of PS-MPs reached 58.46%. HPLC-MS and GC-MS analyses revealed that polystyrene was primarily converted into benzoic acid after degradation, indicating excellent selectivity. Hu et al. [100] synthesized Bi_4NbO_8X (X = Cl, Br) polar single-crystal nanosheets via a molten salt method. The simultaneous application of light illumination and ultrasound significantly increased the production rate of active species (the production rates of $\bullet O_2^-$, H_2O_2, and •OH were 98.7, 792, and 33.2 $\mu mol \cdot g^{-1} \cdot h^{-1}$, respectively), far exceeding those achieved by individual excitation processes. It was determined that these species primarily originated from the oxygen reduction reaction

(ORR). Mechanistic analysis indicated that the polarization field and band bending induced by the piezoelectric potential facilitated bulk charge separation within the catalyst. Benefiting from the increased number of reduction active sites, piezoelectric photo deposition of Pt as a cocatalyst also more efficiently enhanced the photocatalytic hydrogen production activity of Bi_4NbO_8Br compared to conventional photo deposited Pt.

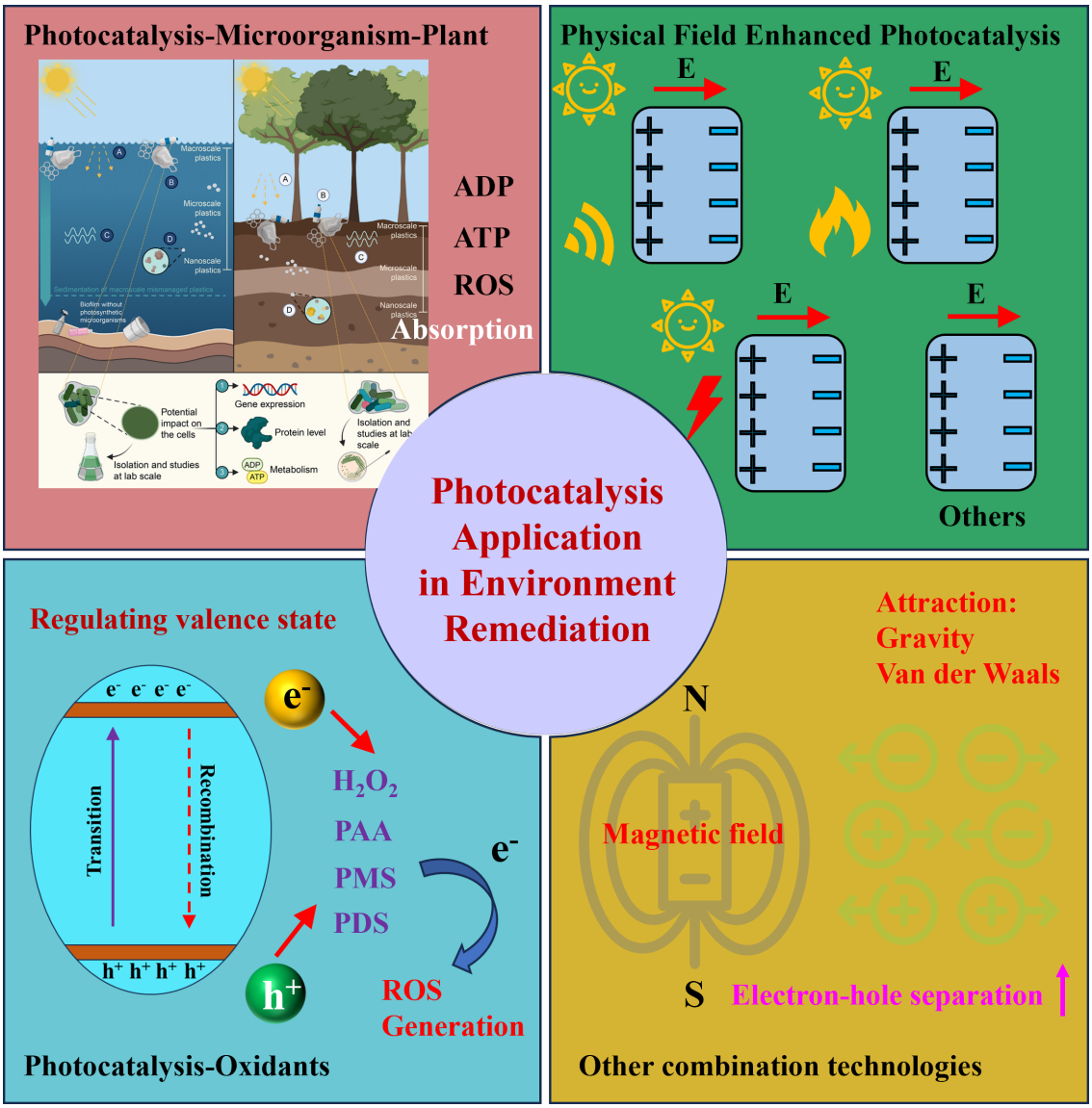

Figure 6. Photocatalysis combined with other biological and physical effects for the appliction in environment remediation.

Considering the high energy consumption associated with ultrasound-mediated catalyst vibration, researchers have developed highly sensitive catalytic materials capable of directly responding to hydraulic disturbances through the piezoelectric effect. For instance, Wang et al. [101] fabricated a ZnO nanorod/PVDF-HFP thin-film composite material. The pollutant removal performance of this material in water significantly improved with increasing rotational speed under different hydraulic conditions. As the hydraulic shear stress intensified (from 200 rpm to 1000 rpm), the reaction rate constant increased from 0.0101 min^{-1} to 0.0399 min^{-1}, with a coupling coefficient between piezoelectric and photoelectric effects as high as 3.83. This study provides valuable insights for developing low-energy photocatalytic treatment processes, demonstrating the potential to directly utilize mechanical energy from existing wastewater treatment operations (such as mixing and aeration) to induce piezoelectric effects for enhanced photocatalytic performance.

Photothermal catalysis and photo-electrocatalysis also provide significant enhancement for photocatalytic reactions under certain conditions [102]. For instance, some photocatalytic reactions are endothermic, and the utilization of photothermal effects can overcome the reaction energy barrier required by thermodynamics, enabling the catalytic process to proceed. In the context of photocatalytic waste plastic degradation and transformation, certain plastics exhibit hydrophobicity, making solid-solid reactions between reactive species generated by the

catalyst and the plastic extremely challenging, resulting in low degradation efficiency [103]. Under photothermal conditions, solid plastic polymers can transition into a molten state within a short period, thereby achieving sufficient contact with the catalyst. Furthermore, in the photocatalytic degradation of organic pollutants, the instantaneous photothermal effect of the catalyst can generate localized high temperatures, which promote the cleavage of chemical bonds in organic molecules in contact with the catalyst surface, thereby enhancing the catalytic reaction rate. Photo-electrocatalytic reactions optimize the quantum efficiency and reaction rate of single photocatalytic systems. The electric field driving force facilitates the separation of photogenerated electron-hole pairs in photocatalytic materials and enhances redox activity.

Furthermore, enhancing mass transfer at the solid-liquid interface through external fields can also improve photocatalytic reaction efficiency. For example, high gravity, slurry systems, spinning disc reactors and monolithic reactors are in the intensification of mass transfer [104]. By applying enhanced gravity to reduce the liquid film thickness at the catalyst interface, when the thickness falls below a critical value (approximately 130 μm), the mass transfer resistance of reactants and products at the solid-liquid interface is significantly reduced, leading to a remarkable improvement in photocatalytic efficiency. However, when the thickness decreases below 60 μm, the enhancement effect of the high-gravity field becomes negligible. When the average liquid film thickness is below the critical value, the rate constant of photocatalytic degradation is proportional to the rotational speed and average radius of the rotating bed, and inversely proportional to the square root of the liquid flow rate and dynamic viscosity. An obvious advantage of these systems is the good contact between reactants and catalyst, scaling up such a device implies a separation step of the catalyst from the reaction products, with major technical and economical problems.

The synergy between photocatalysis and oxidants or magnetic fields also provides theoretical and practical insights for enhancing traditional single photocatalytic technologies. For instance, photoactivation of oxidants such as persulfate, peracetic acid, hydrogen peroxide, and periodate, compared to direct oxidation by oxidants or catalytic reactions, can effectively promote the valence state renewal of metal ions in catalysts through the introduction of light energy, thereby maintaining efficient activation of oxidants and enhancing the degradation efficiency of target pollutants [105]. Photo-magnetic coupling has recently emerged as one of the innovative technologies to enhance photocatalytic reactions [106]. However, due to challenges in controllability, its practical application in environmental remediation remains limited. Under an external magnetic field, the spin states of certain metal ions in photocatalytic materials undergo changes, influencing their electron distribution patterns. Consequently, the migration behavior of photogenerated electrons and holes is affected, leading to variations in photocatalytic activity.

4. LCA of Typical Photocatalytic Technologies

ML methods have been used to generate lifecycle inventories, calculate representation factors, estimate lifecycle impacts, and support lifecycle interpretation. ML models have unique advantages, such as the ability to achieve accurate predictions, discover complex patterns, and effectively analyze large datasets. Firstly, most of the reviewed LCA studies rely on ML's high predictive accuracy to fill missing values in the lifecycle inventory or impact Secondly, machine learning provides novel insights into the driving factors and patterns of environmental performance, which helps decision-makers develop solutions that can improve environmental performance Finally, compared to traditional process based models, ML models exhibit faster execution speeds and are flexibly integrated into other simulation platforms. This effectively solves the problem of evaluation bias caused by missing data in photocatalytic processes using a single LCA.

According to the ISO standard, LCA comprises four fundamental stages: (1) goal and scope definition, wherein the purpose, scope, key assumptions, as well as the types and quality of data are defined [107]. (2) Inventory analysis, which involves data collection to quantify the inputs and outputs of the system. This part faces challenges of information lack, such as toxicity of some by-products, technique details and so on, ML could offer predicted data. (3) Impact assessment, wherein the potential environmental impacts generated by the system under study are identified and characterized. (4) Interpretation, wherein the obtained results are discussed in terms of key sources of impacts and the ways or opportunities to mitigate them [108]. In the context of photocatalytic environmental pollution remediation systems, the entire LCA process can be defined to encompass catalyst synthesis, selection of photocatalytic process, material and energy inputs and outputs, evaluation indicators, and the environmental impact of the process (Figure 7). A detailed elaboration of the photocatalytic LCA process is shown as follows.

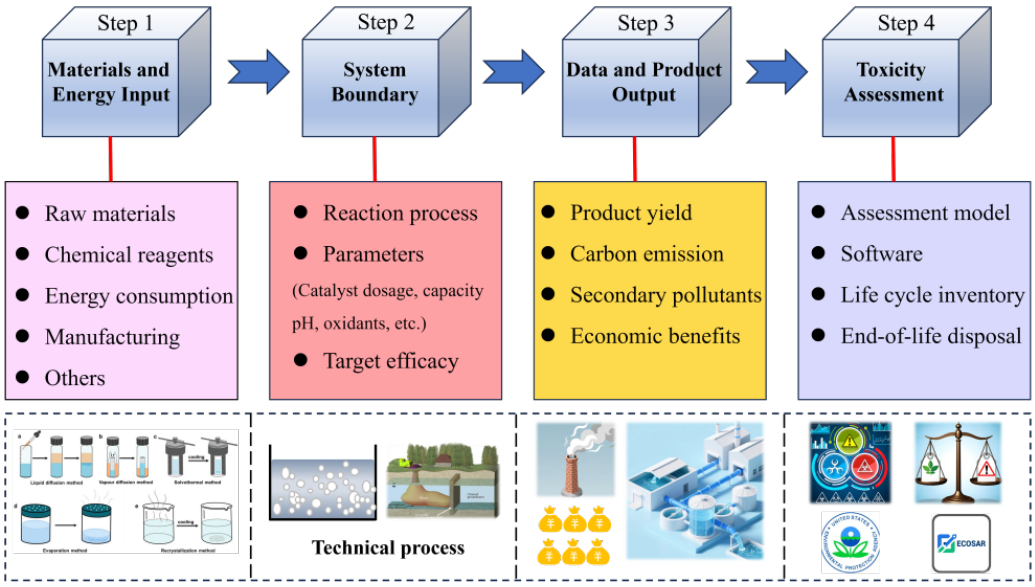

Figure 7. Overall guidance for LCA study of photocatalytic technologies during environmental remediation.

4.1. Technological Process and System Boundary Conditions

Although photocatalytic technology has been extensively studied in the field of environmental pollution remediation, its application costs and environmental impacts have long lacked systematic interpretation, which has hindered its large-scale implementation in practical environmental remediation [109]. By adopting a life cycle assessment framework, it is essential to establish a holistic operational model for photocatalytic technology that encompasses "material synthesis, application processes, target efficacy, waste management, economic benefits, and environmental impacts." This approach will help define clear assessment benchmarks and system boundary conditions, thereby guiding the improvement of photocatalytic processes and promoting their rational application.

For instance, in the context of environmental pollutant remediation, evaluation objectives may include carbon dioxide emissions and the cost per unit volume of pollutants treated, while simultaneously comparing the cost-benefit disparities between the target technology and conventional processes to assess its feasibility. After defining the evaluation objectives, system boundaries are further selected, such as delineating the research scope to include closed-loop systems encompassing material preparation, catalytic reaction processes, secondary pollutant treatment, and catalyst reuse. Comparisons and assessments with other processes are conducted within the same defined boundaries. Suthirat et al. [110] established a LCA framework for the degradation of cyanate in tailings wastewater using UV-TiO_2/$FeCl_3$. The system boundaries encompassed energy inputs (electricity consumption) for three photocatalysis-based experiments (namely UV-A, visible light, and solar radiation), utilization of chemicals and materials (e.g., titanium precursors, ethanol, and hydrochloric acid), and outputs (i.e., emissions to air and water). Energy and chemical consumption for the synthesis of nano-TiO_2/$FeCl_3$ photocatalysts including hydrolysis-polymerization, sol-gel, gelation, evaporation, and calcination were considered. At the treatment endpoint, evaluation indicators included total inorganic carbon (TIC), carbon dioxide, and N_2 production. The study concluded that cyanate removal under visible light irradiation had a marginally greater impact on climate change (34.20%) compared to UV-A (32.99%) and natural solar radiation (32.81%).

In terms of human health impacts, the electricity consumption throughout the life cycle of cyanate photocatalysis accounted for approximately 54.46% of the total human health impacts across all irradiation sources, while the synthesis of nano-TiO_2/ferric chloride photocatalyst contributed 38.71%. Concurrently, ethanol utilization was responsible for over 80% of the total resource depletion. The study indicated that the synthesis process of TiO_2 nanoparticles had the most significant environmental impact, highlighting the need to prioritize green and environmentally friendly synthesis methods to mitigate environmental risks. Alalm et al. [111,112] employed LCA tools to evaluate five solar-based treatment methods: solar photolysis (with and without H_2O_2), photocatalysis using TiO_2 (with and without H_2O_2), and a photo-Fenton reaction system. A pilot-scale compound parabolic collector (CPC) photoreactor was established to determine treatment targets including total organic carbon (TOC) removal, environmental footprint, and material consumption under fixed conditions such as wastewater volume, pollutant concentration, H_2O_2 dosage, and catalyst loading.

The above cases underscore the critical importance of defining clear assessment goals and boundary conditions in LCA. The determination of system boundaries should integrate practical treatment processes and pollution status,

fully accounting for the inputs, outputs, and environmental impacts of process operation to ensure the assessment provides meaningful guidance for real-world applications. ML can assist in obtaining effective data more quickly by training different models and establishing key descriptors in the LCA process. Meanwhile, through multidimensional comparison of big data, it can improve the accuracy of LCA in actual environmental remediation.

4.2. Collection of Experimental Data

Within the defined boundary conditions and evaluation objectives, experimental data from each stage must be collected to determine the life cycle inventory (LCI), outline the full life cycle process, and subsequently assess the carbon emissions, material consumption, cost input, and environmental impact of the photocatalytic reaction [113]. As illustrated, during the material preparation stage, data pertaining to the raw materials, chemical reagents, preparation methods, and energy consumption required for calcination to prepare the photocatalyst need to be gathered. Correspondingly, based on the inventory of material and energy inputs, potentially output substances (e.g., VOCs, CO_2, etc.) should be listed. Silva et al. [114] established a material inventory for photocatalytic reactions, including catalyst dosage, oxidant dosage, acid-base consumption, and wastewater treatment volume, to further analyze toxicity data of secondary wastewater. During the process operation stage, experimental parameters typically involve the electrical energy input for simulating sunlight, catalyst usage, pollutant load, catalyst recovery rate, and pollutant removal rate. For the deactivated catalyst and accompanying secondary pollutants, data on catalyst disposal methods and processes need to be collected to support the assessment of the environmental impact of the photocatalytic process and the costs associated with waste disposal. However, current assessment systems rarely collect information on the concentration and environmental impact of intermediate transformation products of pollutants. Therefore, the LCA framework for photocatalytic systems requires further refinement.

4.3. Environmental Impact and Toxicity Assessment

Current lifecycle assessment methods fail to consistently account for changes throughout the lifecycle, including variations in photocatalytic processes, fluctuations in material supply, and adjustments in policies and regulations. ML can be incorporated into real-time algorithms to assess production or process alterations and propose potential alternatives, thereby enabling more environmentally friendly or less impactful production practices.

To further evaluate the environmental, health, and ecological impacts of photocatalytic treatment systems, Joana et al. utilized SimaPro 9 software to conduct a LCA of photocatalysis. The ReCiPe method was employed for environmental impact assessment, covering impact categories such as global warming, stratospheric ozone depletion, ionizing radiation, ozone formation (human health and terrestrial ecosystems), fine particulate matter formation, terrestrial acidification, freshwater eutrophication, marine eutrophication, terrestrial ecotoxicity, freshwater ecotoxicity, marine ecotoxicity, human toxicity (cancer and non-cancer effects), land use, mineral resource scarcity, fossil resource scarcity, and water consumption. The USEtox model was adopted as a complementary approach to assess toxicity-related categories (human toxicity, freshwater ecotoxicity) for both initial and final effluent. During the impact assessment phase, inventory data were correlated with potential impact categories, and contributions to each category were calculated.

Foteinis et al. [111] selected a photo-Fenton reaction as the research subject and normalized the life cycle inventory (LCI) of each advanced oxidation process (AOP) under study per functional unit to investigate the environmental performance of different technologies. An attributional life cycle assessment (ALCA) was applied because it estimates the environmental impacts of a product or system based on the delivery of functional units. An endpoint or damage-oriented approach translates environmental impacts into areas of concern, such as human health, natural environment, and natural resources. The results indicated that the reagents used in light-driven AOPs (Fe^{2+}, H_2O_2, and H_2SO_4) had relatively low environmental impacts, as these chemicals do not cause adverse health or ecosystem effects, do not generate harmful by-products, and are used only in low doses. In the design phase of photocatalytic processes, it is not easy to obtain a life cycle inventory (LCI) of the process technology. However, these are needed to evaluate whether new chemicals and alternative technologies are environmentally friendly, have long-term sustainability, and are safer when implemented on a large scale. Determining these may be time-consuming through traditional methods such as laboratory experiments, pilot scale studies, computationally intensive molecular simulations, and group contribution methods. To this end, Yinkie et al. [115] proposed machine learning (ML) methods that use data collected from the exploration stage of process development (such as the physical, chemical, molecular, and structural properties of chemicals) as input features to predict LCI. These input features are easily obtainable in well-established chemical databases or can be measured through laboratory experimental techniques. Through machine learning based prediction algorithms such as neural networks and extreme gradient boosting, we can generate LCI data of different categories as output

labels. The combination of LCA and ML provides reference and guidance for the use of photocatalytic technology in environmental remediation, while avoiding interruptions in the evaluation process caused by data loss.

5. Conclusions and Perspectives

With the recent emergence of ML to accelerate the design and discovery of photocatalysts, significant opportunities also exist in developing photocatalytic technologies on environmental applications. In this review, we present a novel perspective on ML assisted comprehensive pathway from catalyst development to the optimization of photocatalysis parameters and a full life cycle assessment process. First, we summarize the powerful capabilities of current ML in the design and synthesis of photocatalysts and the elucidation of reaction mechanisms which will greatly enhance the regulation of catalyst active sites and predict the reaction conditions of catalysts in practical scenarios. Second, we discuss the research and applications of photocatalytic technologies in environmental remediation (water, soil, and air) and highlight several persisting challenges. Finally, we explore the application of LCA to evaluate the entire process of photocatalytic environmental remediation, aiming to provide robust support for process selection and environmental impact evaluation. Based on these discussions, we identify critical focal points and challenges for the future development of photocatalytic technologies.

(i) Lack of detailed description about model selection in photocatalytic process

In the complete photocatalytic process, machine learning is mainly applied to the screening, design, and explanation of reaction mechanisms of front-end photocatalysts, while models for optimizing process conditions and guiding process flow for back-end applications are extremely lacking. At the same time, the various parameters in the photocatalytic reaction process are complex, which makes the computational complexity of many parameters in the machine learning model framework exceptionally large, increasing the uncertainty of the results. In the whole life cycle assessment process of photocatalytic environmental remediation, there are almost no detailed models to guide the determination of assessment details, and it is urgent to propose targeted paradigm references.

(ii) Multimodal Data Fusion and Cross-scale Model

Materials Genome Initiative for Photocatalysts: Integrate experimental data (XRD, XPS), computational data (DFT), and characterization data (such as morphological structure, band structure, light absorption properties, and electron-hole separation capability of photocatalysts) to construct a database for structure-property relationships of photocatalysts. Until now, it is still facing issues such as data dispersion and insufficient physical interpretability of models. In the future, it is necessary to combine high-throughput experiments with multimodal data to develop more interpretable hybrid models, in order to further promote the large-scale application of photocatalytic technology in environmental remediation. Employing ML-based reinforcement learning (RL) to balance activity, stability, and preparation cost in catalyst design. For instance, when aiming to synthesize visible-light-responsive photocatalytic materials for in situ H_2O_2 generation, relevant information on catalyst types, synthesis methods, and optimization strategies can be rapidly retrieved from the database.

(iii) ML-assisted Catalytic Mechanism Analysis

Currently, elucidating the mechanisms of photocatalytic reactions typically involves sophisticated and precise operations, such as catalyst structural characterization, analysis of quantum chemical processes in catalysts, identification of reactive species in the reaction system, and detection of intermediate products during pollutant degradation. Leveraging ML and big data models to achieve predictive and interpretative analysis of reaction processes represents a promising future goal. However, several key challenges remain, including the complex structure-activity relationships of catalysts, insufficient data for big data modeling, and the lack of standardized operational procedures. Therefore, future research should focus on enhancing the following aspects. Integrating attention mechanisms with quantum chemical calculations to dynamically track the evolution pathways of photocatalytic reaction intermediates. The evolution processes of active species should be correlated with target pollutant degradation, byproduct formation, and toxicity information to derive normalized analytical conclusions. Utilizing SHapley Additive exPlanations (SHAP) value analysis to reveal the structure-activity relationship between atomic arrangements on catalyst surfaces and catalytic activity. Based on existing experimental data, ML-based material structure prediction models and volcanic activity models for photocatalytic quantum efficiency should be developed to expand the current big data model repository.

(iv) Goal-Oriented Industrial Application

The application of photocatalytic technology in large-scale environmental remediation remains constrained, primarily due to challenges in mass production of catalysts, issues related to catalyst stability and lifespan, relatively high costs, and the inherent contradiction between catalytic activity, particle size, and practical implementation. Therefore, future research on photocatalytic environmental remediation should shift from

mechanistic studies toward process development, pilot-scale applications, and real-world demonstrations, addressing practical problems encountered in reaction systems through application. For instance, ML can analyze the synergistic effects of complex environmental factors such as aeration, heavy metals, and light. By constructing machine learning models through molecular fingerprints and experimental conditions such as pH, temperature, and catalyst dosage, it can quickly predict the photocatalytic degradation rate of organic pollutants.

(v) Carbon Neutrality-Oriented Green Design

Predicting the life-cycle carbon emissions of photocatalysts through ML models, encompassing synthesis, usage, and post-treatment stages, to guide the selection of low-energy synthesis pathways. simultaneously, employing ML-assisted design of recyclable catalysts (e.g., magnetic nanomaterials), large-particle photocatalysts, membrane materials, and gel materials to enhance environmental friendliness.

Author Contributions

W.L.: conceptualization, writing-original draft preparation, data collection; B.W.: conceptualization, data collection; D.Y.: visualization; S.Z.: supervision, reviewing. All authors have read and agreed to the published version of the manuscript.

Funding

This research was funded by the National Key Research and Development Program of China (2024YFC3908500), the National Natural Science Foundation of China (Grant Nos. 22225604, and U24A20518), Tianjin Commission of Science and Technology as key technologies R&D projects (23YFZCSN00010), the Frontiers Science Center for New Organic Matter (Grant No. 63181206), and Haihe Laboratory of Sustainable Chemical Transformations.

Institutional Review Board Statement

Not applicable.

Informed Consent Statement

Not applicable.

Acknowledgments

The authors gratefully acknowledge the financially support by the National Key Research and Development Program of China (2024YFC3908500), the National Natural Science Foundation of China (Grant Nos. 22225604, and U24A20518), Tianjin Commission of Science and Technology as key technologies R&D projects (23YFZCSN00010), the Frontiers Science Center for New Organic Matter (Grant No. 63181206), and Haihe Laboratory of Sustainable Chemical Transformations.

Conflicts of Interest

The authors declare no conflict of interest.

Use of AI and AI-Assisted Technologies

No AI tools were utilized for this paper.

Reference

1. Asghar, H.; Saeed, M.; Mirsafi, F.S.; et al. Zinc Oxide-Graphitic Carbon Nitride Composites: Synthesis, Properties, and Application Scopes in Environmental Remediations. *Small* **2025**, *21*, e09637.
2. Li, S.; Zhang, T.; Zheng, H.; et al. Efficient photo-Fenton degradation of water pollutants via peracetic acid activation over sulfur vacancies-rich metal sulfides/MXenes. *Appl. Cataly. B-Environ. Energy* **2025**, *366*, 125000.
3. Lv, M.; Liu, Y.; Wang, M.; et al. Transformative Forces: The Role of Gut Microbiota in Processing Environmental Pollutants. *Environ. Sci. Technol.* **2025**, *59*, 15575–15593.
4. Gao, X.; Zheng, X.; Wang, X.; et al. Environmental pollutant exposure and adverse neurodevelopmental outcomes: An umbrella review and evidence grading of meta-analyses. *J. Hazard. Mater.* **2025**, *491*, 137832.
5. Pirvu, F.; Pascu, L.F.; Paun, I.; et al. Sorption of PAHs onto microplastics in Romanian surface waters and sediments:

Environmental toxicity and human health risk with emphasis on pediatric exposure. *Water Res.* **2025**, *287*, 124483.
6. Yu, X.; Tang, L.; Yan, R.; et al. Quantifying PFAS contamination and environmental risk in municipal solid waste landfill refuse: Implications for landfill reuse. *Water Res.* **2025**, *283*, 123881.
7. Wang, H.; Zhang, S.; Lin, Z.; et al. Occurrence, removal and ecological risk assessment of antibiotics in rural domestic wastewater treatment systems in the Beijing-Tianjin-Hebei region. *J. Hazard. Mater.* **2025**, *495*, 139127.
8. Cui, P.; Schito, G.; Cui, Q. VOC emissions from asphalt pavement and health risks to construction workers. *J. Clean. Prod.* **2020**, *244*, 118757.
9. Liu, J.; Qi, W.; Xu, M.; et al. Piezocatalytic Techniques in Environmental Remediation. *Angew. Chem. Int. Ed.* **2023**, *62*, e202213927.
10. Zadehnazari, A.; Khosropour, A.; Zarei, A.; et al. Viologen-Derived Covalent Organic Frameworks: Advancing PFAS Removal Technology with High Adsorption Capacity. *Small* **2024**, *20*, 2405176.
11. Xiang, J.; Zhou, Z.; Liu, Z.; et al. Constructing simplified microbial consortia that couple lactic acid and ethanol utilization to highly produce caproic acid from liquor-making wastewater. *Water Res.* **2025**, *284*, 123973.
12. Dicataldo, G.; Desmond, P.; Al-Maas, M.; et al. Feasibility and application of membrane aerated biofilm reactors for industrial wastewater treatment. *Water Res.* **2025**, *280*, 123523.
13. Wang, C.; Qi, W.-K.; Zhang, S.-J.; et al. Innovation for continuous aerobic granular sludge process in actual municipal sewage treatment: Self-circulating up-flow fluidized bed process. *Water Res.* **2024**, *260*, 121862.
14. Wang, S.; Song, W.; Liu, E.; et al. Efficient, facile and recyclable coating strategy to improve heavy metals removal by UF membrane in drinking water purification. *Sep. Purif. Technol.* **2025**, *363*, 131995.
15. Wang, X.; Guo, S.; Chen, W.; et al. Fe_2O_3-Kao@g-CN activated peroxymonosulfate remediation of bensulfuron methyl-polluted water and soil: Detoxification, soil properties and crop growth. *Chem. Eng. J.* **2024**, *487*, 150745.
16. Kasula, M.; Ortbal, S.; Kebede, M.M.; et al. Evaluating Biofiltration Pretreatment and NOM-PFAS Dynamics in PFAS Removal by Nanofiltration Membranes. *ACS EST Water* **2025**, *5*, 3628–3642.
17. Hou, L.; Hu, K.; Huang, F.; et al. Advances in immobilized microbial technology and its application to wastewater treatment: A review. *Bioresour. Technol.* **2024**, *413*, 131518.
18. Su, H.; Yin, H.; Wang, R.; et al. Atomic-level coordination structures meet graphitic carbon nitride (g-C_3N_4) for photocatalysis: Energy conversion and environmental remediation. *Appl. Catal. B-Environ. Energy* **2024**, *348*, 123683.
19. Wakjira, T.L.; Gemta, A.B.; Kassahun, G.B.; et al. Bismuth-Based Z-Scheme Heterojunction Photocatalysts for Remediation of Contaminated Water. *ACS Omega* **2024**, *9*, 8709–8729.
20. Wang, W.; Zhang, W.; Deng, C.; et al. Accelerated Photocatalytic Carbon Dioxide Reduction and Water Oxidation under Spatial Synergy. *Angew. Chem. Int. Ed.* **2024**, *63*, e202317969.
21. Xu, D.; Wang, H.; Zhang, K.; et al. Photocatalytic Waste Polystyrene Plastic Conversion: Reaction Mechanism and Catalyst Design. *Environ. Sci. Technol.* **2025**, *59*, 16112–16129.
22. Mani, S.S.; Rajendran, S.; Mathew, T.; et al. A review on the recent advances in the design and structure–activity relationship of TiO_2-based photocatalysts for solar hydrogen production. *Energy Adv.* **2024**, *3*, 1472–1504.
23. Tian, T.; Lu, D.; Zhao, B.; et al. Exploring the intrinsic relationship between defects in g-C_3N_4 and the enhancement of photogenerated carrier dynamics and photocatalytic performance. *J. Alloys Compd.* **2025**, *1010*, 178135.
24. Zheng, X.; Song, Y.; Gao, Q.; et al. Controllable-Photocorrosion Balance Endows ZnCdS Stable Photocatalytic Hydrogen Evolution. *Adv. Funct. Mater.* **2025**, *35*, 2506159.
25. Zhang, X.; Bo, C.; Cao, S.; et al. Stability improvement of a Pt/TiO_2 photocatalyst during photocatalytic pure water splitting. *J. Mater. Chem. A* **2022**, *10*, 24381–24387.
26. Masood, H.; Toe, C.Y.; Teoh, W.Y.; et al. Machine Learning for Accelerated Discovery of Solar Photocatalysts. *ACS Catal.* **2019**, *9*, 11774–11787.
27. Shiekhmohammadi, A.; Alamgholiloo, H.; Asgari, E.; et al. A plasmonic S-scheme Ag/ZrO_2/TCN photocatalyst for enhancing interfacial charge transfer: Insights to machine learning models and mechanism for photodegradation. *Colloids Surf. A* **2025**, *717*, 136858.
28. Wayo, D.D.K.; Goliatt, L.; Ganji, M.D.; et al. DFT and hybrid classical–quantum machine learning integration for photocatalyst discovery and hydrogen production. *Rev. Chem. Eng.* **2025**, *41*, 741–774.
29. Tunala, S.; Zhai, S.; Wu, F.; et al. Machine learning in photocatalysis: Accelerating design, understanding, and environmental applications. *Sci. China Chem.* **2025**, *68*, 3415–3428.
30. Li, X.; Maffettone, P.M.; Che, Y.; et al. Combining machine learning and high-throughput experimentation to discover photocatalytically active organic molecules. *Chem. Sci.* **2021**, *12*, 10742–10754.
31. Mai, H.; Le, T.C.; Chen, D.; et al. Machine Learning for Electrocatalyst and Photocatalyst Design and Discovery. *Chem. Rev.* **2022**, *122*, 13478–13515.
32. Wang, S.; Mo, P.; Li, D.; et al. Intelligent Algorithms Enable Photocatalyst Design and Performance Prediction. *Catalysts* **2024**, *14*, 217.

33. Xiao, Y.; Choudhuri, K.; Thanetchaiyakup, A.; et al. Machine-Learning-Assisted Discovery of Mechanosynthesized Lead-Free Metal Halide Perovskites for the Oxidative Photocatalytic Cleavage of Alkenes. *Adv. Sci.* **2024**, *11*, 2309714.
34. Pang, Y.; Li, P.; Ma, X.; et al. Metal-doped carbon nitride: An all-in-one photocatalyst. *EES Catal.* **2023**, *1*, 810–831.
35. Wang, L.; Kong, Y.; Fang, Y.; et al. A Ga Doped $NiTiO_3$ Photocatalyst for Overall Water Splitting under Visible Light Illumination. *Adv. Funct. Mater.* **2022**, *32*, 2208101.
36. Tu, B.; Hao, J.; Wang, F.; et al. Element doping adjusted the built-in electric field at the TiO_2/CdS interface to enhance the photocatalytic reduction activity of Cr(VI). *Chem. Eng. J.* **2023**, *456*, 141103.
37. Ye, L.; Jin, X.; Liu, C.; et al. Thickness-ultrathin and bismuth-rich strategies for BiOBr to enhance photoreduction of CO_2 into solar fuels. *Appl. Catal. B-Environ. Energy* **2016**, *187*, 281–290.
38. Bai, Y.; Wilbraham, L.; Slater, B.J.; et al. Accelerated Discovery of Organic Polymer Photocatalysts for Hydrogen Evolution from Water through the Integration of Experiment and Theory. *J. Am. Chem. Soc.* **2019**, *141*, 9063–9071.
39. Wang, Y.; Kang, Y.; Zhu, H.; et al. Perovskite Oxynitride Solid Solutions of $LaTaON_2$-$CaTaO_2N$ with Greatly Enhanced Photogenerated Charge Separation for Solar-Driven Overall Water Splitting. *Adv. Sci.* **2021**, *8*, 2003343.
40. Xiao, M.; Wang, Z.; Lyu, M.; et al. Hollow Nanostructures for Photocatalysis: Advantages and Challenges. *Adv. Mater.* **2019**, *31*, 1801369.
41. Wang, Z.; Gu, Y.; Zheng, L.; et al. Machine Learning Guided Dopant Selection for Metal Oxide-Based Photoelectrochemical Water Splitting: The Case Study of Fe_2O_3 and CuO. *Adv. Mater.* **2022**, *34*, 2106776.
42. Nishimura, T.; Kumabe, Y.; Harashima, Y.; et al. Machine-Learning-Driven Photocurrent Prediction in Multielement-Doped Hematite Photoelectrodes. *ACS Catal.* **2025**, *15*, 11993–12004.
43. Zhang, L.; Chen, G.X.; Wang, Z.L.; et al. Automated machine learning guides discovery of ABO_3-type oxides for effective water splitting photocatalysis. *Chem. Phys. Lett.* **2025**, *869*, 142034.
44. Sohrabi, S.; Rahimi, P.; Khedri, M.; et al. Evaluation of machine learning and molecular dynamics models for photocatalytic water decontamination. *Process Saf. Environ. Prot.* **2025**, *195*, 106780.
45. Mai, H.; Li, X.; Le, T.C.; et al. Rapid Design of Efficient Mn_3O_4-Based Photocatalysts by Machine Learning and Density Functional Theory Calculations. *Adv. Energy Sustain. Res.* **2025**, *6*, 2400397.
46. Wang, H.; You, C. Photocatalytic oxidation of SO_2 on TiO_2 and the catalyst deactivation: A kinetic study. *Chem. Eng. J.* **2018**, *350*, 268–277.
47. Haselmann, G.M.; Eder, D. Early-Stage Deactivation of Platinum-Loaded TiO_2 Using In Situ Photodeposition during Photocatalytic Hydrogen Evolution. *ACS Catal.* **2017**, *7*, 4668–4675.
48. Weon, S.; Choi, W. TiO_2 Nanotubes with Open Channels as Deactivation-Resistant Photocatalyst for the Degradation of Volatile Organic Compounds. *Environ. Sci. Technol.* **2016**, *50*, 2556–2563.
49. Allam, O.; Maghsoodi, M.; Jang, S.S.; et al. Unveiling Competitive Adsorption in TiO_2 Photocatalysis through Machine-Learning-Accelerated Molecular Dynamics, DFT, and Experimental Methods. *ACS Appl. Mater. Interfaces* **2024**, *16*, 36215–36223.
50. Wu, C.H.; Wu, C.F.; Shr, J.F.; et al. Parameter settings on preparation of composite photocatalysts for enhancement of adsorption/photocatalysis hybrid capability. *Sep. Purif. Technol.* **2008**, *61*, 258–265.
51. Fu, X.; Huang, D.; Qin, Y.; et al. Effects of preparation method on the microstructure and photocatalytic performance of $ZnSn(OH)_6$. *Appl. Catal. B* **2014**, *148*, 532–542.
52. Lin, X.; Du, X.; Wu, S.; et al. Machine learning-assisted dual-atom sites design with interpretable descriptors unifying electrocatalytic reactions. *Nat. Commun.* **2024**, *15*, 8169.
53. Li, R. Latest progress in hydrogen production from solar water splitting via photocatalysis, photoelectrochemical, and photovoltaic-photoelectrochemical solutions. *Chin. J. Catal.* **2017**, *38*, 5–12.
54. Wang, Z.; Huang, X.; Wang, X. Recent progresses in the design of $BiVO_4$-based photocatalysts for efficient solar water splitting. *Catal. Today* **2019**, *335*, 31–38.
55. Yao, T.; An, X.; Han, H.; et al. Photoelectrocatalytic Materials for Solar Water Splitting. *Adv. Energy Mater.* **2018**, *8*, 1800210.
56. Huang, M.; Wang, S.; Zhu, H. A comprehensive machine learning strategy for designing high-performance photoanode catalysts. *J. Mater. Chem. A* **2023**, *11*, 21619–21627.
57. Zhang, L.; Zhang, J.; Yu, J.; et al. Charge-transfer dynamics in S-scheme photocatalyst. *Nat. Rev. Chem.* **2025**, *9*, 328–342.
58. Sudrajat, H.; Nobatova, M. Heterojunction photocatalysts: Where are they headed? *RSC Appl. Interfaces* **2025**, *2*, 599–619.
59. Wang, Z.; Li, C.; Domen, K. Recent developments in heterogeneous photocatalysts for solar-driven overall water splitting. *Chem. Soc. Rev.* **2019**, *48*, 2109–2125.
60. Zhou, H.; Sheng, X.; Ding, Z.; et al. Liquid–Liquid–Solid Triphase Interface Microenvironment Mediates Efficient Photocatalysis. *ACS Catal.* **2022**, *12*, 13690–13696.
61. Pan, S.; Lu, D.; Gan, H.; et al. Long-range hydrophobic force enhanced interfacial photocatalysis for the submerged surface anti-biofouling. *Water Res.* **2023**, *243*, 120383.
62. Zeng, Z.; Tan, L.; Ye, F.; et al. Carbon nitride with water soluble ability: Enhanced oxygen species interphase mass

transfer for homogenous photocatalytic water purification. *Appl. Surf. Sci.* **2024**, *652*, 159352.
63. Li, L.; Xu, L.; Hu, Z.; et al. Enhanced Mass Transfer of Oxygen through a Gas–Liquid–Solid Interface for Photocatalytic Hydrogen Peroxide Production. *Adv. Funct. Mater.* **2021**, *31*, 2106120.
64. Zhang, G.; Li, X.; Chen, D.; et al. Internal Electric Field and Adsorption Effect Synergistically Boost Carbon Dioxide Conversion on Cadmium Sulfide@Covalent Triazine Frameworks Core–Shell Photocatalyst. *Adv. Funct. Mater.* **2023**, *33*, 2308553.
65. Yu, L.; Wang, Q.; Zhuang, C.; et al. Periodic Frustrated Lewis Pairs on Bimetallic Oxide Semiconductors for CO_2 Adsorption and Photocatalytic Conversion. *ACS Nano* **2025**, *19*, 7239–7252.
66. El-Alami, W.; Sousa, D.G.; González, J.D.; et al. TiO_2 and F-TiO_2 photocatalytic deactivation in gas phase. *Chem. Phys. Lett.* **2017**, *684*, 164–170.
67. Yu, G.; Wang, N. Gas-Liquid-Solid interface enhanced photocatalytic reaction in a microfluidic reactor for water treatment. *Appl. Catal. A* **2020**, *591*, 117410.
68. Zhao, Y.; Guo, J.; Yang, B.; et, al. A multilayered Co–Fe MOF/GO 3D evaporator for efficient solar-driven water generation and wastewater purification. *J. Mater. Chem. A* **2025**, *13*, 27314–27325.
69. Wang, W.; Tian, Z.; Huan, X.; et al. Solar-Driven Interfacial Evaporation: Material Types, Structural Strategies, and Emerging Applications. *Langmuir* **2025**, *41*, 24097–24134.
70. Song, Y.; Fang, S.; Xu, N.; et al. Solar-driven interfacial evaporation technologies for food, energy and water. *Nat. Rev. Clean. Technol.* **2025**, *1*, 55–74.
71. Lv, B.; Dong, X.; Xu, Y.; et al. A self-sufficient catalytic nanofiber evaporator for solar-driven efficient water purification through in-situ hydrogen peroxide generation. *Chem. Eng. J.* **2024**, *501*, 157611.
72. Sheng, X.; Liu, Z.; Zeng, R.; et al. Enhanced Photocatalytic Reaction at Air–Liquid–Solid Joint Interfaces. *J. Am. Chem. Soc.* **2017**, *139*, 12402–12405.
73. Chen, R.; Li, J.; Wang, H.; et al. Photocatalytic reaction mechanisms at a gas–solid interface for typical air pollutant decomposition. *J. Mater. Chem. A* **2021**, *9*, 20184–20210.
74. Ma, H.; Wang, X.; Jin, R.; et al. Promote hydroxyl radical and key intermediates formation for deep toluene mineralization via unique electron transfer channel. *J. Colloid Interface Sci.* **2023**, *630*, 704–713.
75. Li, Y.; Ouyang, S.; Xu, H.; et al. Constructing Solid–Gas-Interfacial Fenton Reaction over Alkalinized-C_3N_4 Photocatalyst To Achieve Apparent Quantum Yield of 49% at 420 nm. *J. Am. Chem. Soc.* **2016**, *138*, 13289–13297.
76. Chen, Z.; Zhao, J.; Zhao, J.; et al. Frustrated Lewis pairs photocatalyst for visible light-driven reduction of CO to multi-carbon chemicals. *Nanoscale* **2019**, *11*, 20777–20784.
77. Xu, C.; Yang, W.; Guo, Q.; et al. Photoinduced decomposition of acetaldehyde on a reduced TiO_2(110) surface: Involvement of lattice oxygen. *Phys. Chem. Chem. Phys.* **2016**, *18*, 30982–30989.
78. Lopez-Besora, J.; Pardal, C.; Isalgue, A.; et al. Exploring the Integration of a Novel Photocatalytic Air Purification Façade Component in Buildings. *Buildings* **2024**, *14*, 2481.
79. Asadi, S.; Hassan, M.; Nadiri, A.; et al. Artificial intelligence modeling to evaluate field performance of photocatalytic asphalt pavement for ambient air purification. *Environ. Sci. Pollut. Res.* **2014**, *21*, 8847–8857.
80. Li, W.; Yue, F.; Shi, M.; et al. Thermally assisted photocatalytic industrial flue gas CO_2 conversion: 100% selective CO production via synergistic adsorption–conversion in NH_2–MXene–MOF hierarchical interfaces. *J. Mater. Chem. A* **2025**, *13*, 33233–33244.
81. Murgolo, S.; Franz, S.; Arab, H.; et al. Degradation of emerging organic pollutants in wastewater effluents by electrochemical photocatalysis on nanostructured TiO_2 meshes. *Water Res.* **2019**, *164*, 114920.
82. Ding, R.; Yan, W.; Wu, Y.; et, al. Light-excited photoelectrons coupled with bio-photocatalysis enhanced the degradation efficiency of oxytetracycline. *Water Res.* **2018**, *143*, 589–598.
83. Liu, W.; Dong, Y.; Liu, J.; et al. Halloysite nanotube confined interface engineering enhanced catalytic oxidation of photo-Fenton reaction for aniline aerofloat degradation: Defective heterojunction for electron transfer regulation. *Chem. Eng. J.* **2023**, *451*, 138666.
84. Liu, R.; Zheng, Z.; Spurgeon, J.; et al. Enhanced photoelectrochemical water-splitting performance of semiconductors by surface passivation layers. *Energy Environ. Sci.* **2014**, *7*, 2504–2517.
85. Li, J.; Wei, J.; Sun, J.; et al. Building the bimetallic site of $Co_2Mo_3O_8$/Co_9S_8 heterojunction via interface electronic reconfiguration to enhance peroxymonosulfate activation for singlet oxygen formation. *Chem. Eng. J.* **2025**, *505*, 159739.
86. Kuddushi, M.; Deng, X.; Nayak, J.; et al. A Transparent, Tough and Self-Healable Biopolymeric Composites Hydrogel for Open Wound Management. *ACS Appl. Bio Mater.* **2023**, *6*, 3810–3822.
87. Xu, B.B.; Zhou, M.; Ye, M.; et al. Cooperative Motion in Water–Methanol Clusters Controls the Reaction Rates of Heterogeneous Photocatalytic Reactions. *J. Am. Chem. Soc.* **2021**, *143*, 10940–10947.
88. Mudhoo, A.; Bhatnagar, A.; Rantalankila, M.; et al. Endosulfan removal through bioremediation, photocatalytic degradation, adsorption and membrane separation processes: A review. *Chem. Eng. J.* **2019**, *360*, 912–928.

89. Fazey, F.M.; Ryan, P.G. Debris size and buoyancy influence the dispersal distance of stranded litter. *Mar. Pollut. Bull.* **2016**, *110*, 371–377.
90. Barone, G.D.; Rodríguez-Seijo, A.; Parati, M.; et al. Harnessing photosynthetic microorganisms for enhanced bioremediation of microplastics: A comprehensive review. *Environ. Sci. EcoTechnol.* **2024**, *20*, 100407.
91. Hu, C.; Tu, S.; Tian, N.; et al. Photocatalysis Enhanced by External Fields. *Angew. Chem. Int. Ed.* **2021**, *60*, 16309–16328.
92. Li, X.; Wang, W.; Dong, F.; et al. Recent Advances in Noncontact External-Field-Assisted Photocatalysis: From Fundamentals to Applications. *ACS Catal.* **2021**, *11*, 4739–4769.
93. Zhu, Y.; Wang, H.; Wang, B.; et al. Solar thermoelectric field plus photocatalysis for efficient organic synthesis exemplified by toluene to benzoic acid. *Appl. Catal. B-Environ. Energy* **2016**, *193*, 151–159.
94. Van Doorslaer, X.; Demeestere, K.; Heynderickx, P.M.; et al. Heterogeneous photocatalysis of moxifloxacin: Identification of degradation products and determination of residual antibacterial activity. *Appl. Catal. B-Environ. Energy* **2013**, *138*, 333–341.
95. Zhang, Y.; Qi, M.Y.; Tang, Z.R.; et al. Photoredox-Catalyzed Plastic Waste Conversion: Nonselective Degradation versus Selective Synthesis. *ACS Catal.* **2023**, *13*, 3575–3590.
96. Chen, W.; Li, X.; Wang, F.; et al. Nonepitaxial Gold-Tipped ZnSe Hybrid Nanorods for Efficient Photocatalytic Hydrogen Production. *Small* **2020**, *16*, 1902231.
97. Wu, S.; Quan, X. Design Principles and Strategies of Photocatalytic H_2O_2 Production from O_2 Reduction. *ACS ES&T Eng.* **2022**, *2*, 1068–1079.
98. Xia, C.; Yuan, L.; Song, H.; et al. Spatial Specific Janus S-Scheme Photocatalyst with Enhanced H_2O_2 Production Performance. *Small* **2023**, *19*, 2300292.
99. Lu, Y.; Dong, Y.; Liu, W.; et, al. Piezo-photocatalytic enhanced microplastic degradation on hetero-interpenetrated $Fe_{1-x}S/FeMoO_4/MoS_2$ by producing H_2O_2 and self-Fenton action. *Chem. Eng. J.* **2025**, *508*, 160935.
100. Hu, C.; Huang, H.; Chen, F.; et al. Coupling Piezocatalysis and Photocatalysis in Bi_4NbO_8X (X = Cl, Br) Polar Single Crystals. *Adv. Funct. Mater.* **2020**, *30*, 1908168.
101. Wang, R.; Xie, X.; Xu, C.; et al. Bi-piezoelectric effect assisted ZnO nanorods/PVDF-HFP spongy photocatalyst for enhanced performance on degrading organic pollutant. *Chem. Eng. J.* **2022**, *439*, 135787.
102. Chen, R.; Wang, J.; Zhang, C.; et al. Purification and Value-Added Conversion of NOx under Ambient Conditions with Photo-/Electrocatalysis Technology. *Environ. Sci. Technol.* **2025**, *59*, 1013–1033.
103. Singh, S.; Kapoor, S.; Singh, J.P. Synergistic Photocatalysis by α-MoO_3 Nanostructures and SWCNT Nanocomposites for Efficient Cross-Linking and Oxidative Degradation of Polystyrene Nanoplastics. *ACS Appl. Mater. Interfaces* **2024**, *16*, 40914–40926.
104. Van Gerven, T.; Mul, G.; Moulijn, J.; et al. A review of intensification of photocatalytic processes. *Chem. Eng. Process* **2007**, *46*, 781–789.
105. Jiang, H.; Chen, H.; Fu, Y.; et al. $SnFe_2O_4$ mediated near-infrared-driven photocatalysis, photothermal sterilization and piezocatalysis. *Appl. Surf. Sci.* **2023**, *611*, 155555.
106. Lu, D.; Ren, Y.; Yang, Y.; et al. Boosted photocatalytic CO_2 reduction by induced electromotive force in rotating magnetic field. *Nano Energy* **2023**, *113*, 108578.
107. Gong, Y.N.; Zhong, D.C.; Lu, T.B. Porous Supramolecular Crystalline Materials for Photocatalysis. *Angew. Chem. Int. Ed.* **2025**, *64*, e202424452.
108. Munoz, I.; Rieradevall, J.; Torrades, F.; et al. Environmental assessment of different solar driven advanced oxidation processes. *Sol. Energy* **2005**, *79*, 369–375.
109. Muñoz, I.; Peral, J.; Ayllón, J.A.; et al. Life cycle assessment of a coupled solar photocatalytic–biological process for wastewater treatment. *Water Res.* **2006**, *40*, 3533–3540.
110. Dubsok, A.; Khamdahsag, P.; Kittipongvises, S. Life cycle environmental impact assessment of cyanate removal in mine tailings wastewater by nano-$TiO_2/FeCl_3$ photocatalysis. *J. Clean. Prod.* **2022**, *366*, 132928.
111. Foteinis, S.; Borthwick, A.G.; Frontistis, Z.; et al. Environmental sustainability of light-driven processes for wastewater treatment applications. *J. Clean. Prod.* **2018**, *182*, 8–15.
112. Magdy, M.; Alalm, M.G.; El-Etriby, H.K. Comparative life cycle assessment of five chemical methods for removal of phenol and its transformation products. *J. Clean. Prod.*, **2021**, *291*, 125923.
113. Dominguez, S.; Laso, J.; Margallo, M.; et al. LCA of greywater management within a water circular economy restorative thinking framework. *Sci. Total Environ.* **2018**, *621*, 1047–1056.
114. Pesqueira, J.F.; Pereira, M.F.R.; Silva, A.M. A life cycle assessment of solar-based treatments (H_2O_2, TiO_2 photocatalysis, circumneutral photo-Fenton) for the removal of organic micropollutants. *Sci. Total Environ.* **2021**, *761*, 143258.
115. Aboagye, E.; Longo, J.; Conway, M.; et al. Leveraging machine learning algorithms to predict life cycle inventory assessments (LCIA) to facilitate sustainable process design. *Comput. Chem. Eng.* **2025**, *201*, 109217.